

Stochastic oscillations induced by intrinsic fluctuations in a self-repressing gene: a deterministic approach.

Jingkui Wang

Laboratoire de Physique des Lasers, Atomes, et Molécules, CNRS, UMR8523
Université Lille 1, F-59655 Villeneuve d'Ascq, France

Marc Lefranc

Laboratoire de Physique des Lasers, Atomes, et Molécules, CNRS, UMR8523
Université Lille 1, F-59655 Villeneuve d'Ascq, France

Quentin Thommen¹

Laboratoire de Physique des Lasers, Atomes, et Molécules, CNRS, UMR8523
Université Lille 1, F-59655

¹Corresponding author. Address: quentin.thommen@univ-lille1.fr

Abstract

Biochemical reaction networks are subjected to large fluctuations attributable to small molecule numbers, yet underlie reliable biological functions. Most theoretical approaches describe them as purely deterministic or stochastic dynamical systems, depending on which point of view is favored. Here, we investigate the dynamics of a self-repressing gene using an intermediate approach based on a moment closure approximation of the master equation, which allows us to take into account the binary character of gene activity. We thereby obtain deterministic equations that describe how nonlinearity feeds back fluctuations into the mean-field equations, providing insight into the interplay of determinism and stochasticity. This allows us to identify regions of parameter space where fluctuations induce relatively regular oscillations.

Key words: Stochastic gene expression; Self-repressing gene; Genetic oscillations; Master equation; Moment closure; *Hes1*

Introduction

Most cellular functions are controlled by molecular networks involving genes and proteins which regulate each other so as to generate the adequate dynamical behavior. A major goal of systems biology is to understand how sophisticated functional modules emerge from the combination of elementary processes such as transcriptional regulation, complex degradation, active transport,... and how each of these processes influences the collective dynamics (1).

A specificity of regulatory networks viewed as dynamical systems is that they are both strongly nonlinear and inherently stochastic, which considerably complicates the mathematical analysis. In a cell, protein and mRNA molecules are often found in low abundance so that variations of their copy numbers by one unit represent significant fluctuations. Furthermore, DNA fragments carrying genes are single-copy molecules which have only a few possible configurations depending on promoter occupancy. When its transcription is regulated by a single protein, a gene can essentially be in two states: free, or bound to its transcription factor. Gene activity is then be described mathematically by a binary variable, which more generally can also account for the transcriptional pulsing that has been observed both in prokaryotes (2) and eukaryotes (3–6). The stochastic dynamics of the gene randomly flipping between the bound and free states with probabilities depending on transcription factor abundance is a major source of intrinsic fluctuations, all the more at it was shown that this flipping can occur at time scales which are comparable to other biochemical processes (2). While stochasticity in gene networks has been often viewed as an undesirable perturbation blurring deterministic behavior, it is increasingly recognized that noise can in fact be harnessed so as to become a functional component of a regulatory network and make its dynamics richer (7–11). It is thus important to understand how the deterministic and stochastic aspects of cellular processes interact and contribute to the same global dynamics, all the more as they are intimately coupled in nonlinear systems.

However, even moderately complex regulatory networks resist mathematical analysis and require formidable computational resources. A natural strategy to study such general questions as the interplay of dynamics and noise is to focus on small genetic networks comprising only a few elementary components, whose analysis can identify the key mechanisms and parameters and cast light on the dynamics of more complex networks. This approach is all the more valuable as the recent developments of synthetic biology allow experimental tests of the theoretical analyses (12).

Here, we study how stochastic fluctuations in gene activity feed back into the deterministic dynamics of the smallest genetic network, which consists of a single gene repressed by its own protein. This system is an ideal workbench to investigate how the dynamics of the network emerges from the properties of its elementary components. In fact, this motif is very common in transcriptional networks and is thus biologically relevant (around 40% of *Escherichia coli* transcription factors are self-repressing (13–15)). Self-repression is known to be an important ingredient for generating oscillatory behavior (16). For instance, Hirata *et al* proposed that the somite clock network is governed by the self-repressing gene *Hes1* (17). Accordingly, the dynamics

of the self-repressing gene has been actively investigated throughout mathematical biology (18–26).

Most theoretical analyses of the self-repressing gene based on a deterministic description assume that gene state flipping occurs on much faster time scales than other processes such as transcription, translation, and degradation. The flipping dynamics can then be taken into account through an average activity, which adapts to protein concentration either instantaneously or after a time delay. If intrinsic fluctuations are neglected, the analysis of the rate equations reveals that oscillatory behavior can only be found by either (1) introducing an explicit time delay in the equations (e.g., to take into account the transcriptional dynamics (16, 23–25, 27, 28)); (2) inducing an implicit time delay via a reactional step, which can be intrinsic (20) or describe transport between two compartments (22); (3) incorporating complex degradation mechanisms (16, 26, 28, 29). However, recent experiments have shown that gene activity may display an intrinsic dynamics on time scales comparable to that of other cellular processes (2, 4–6). This may be taken into account in a deterministic model by introducing a average gene activity variable, which reacts gradually to protein concentration (30). In particular, how such a transcriptional delay and a nonlinear degradation mechanism conspire to generate oscillations has been studied in detail by Morant *et al.* (26), who obtained analytical expressions for the instability thresholds.

To take into account the binary nature of gene state and its stochasticity, the most general approach to study the dynamics of the self-repressing gene is to use the chemical master equation (CME) (31). The steady-state solution of the CME provides the probability distribution of molecular copy numbers, characterizing both the averages and the fluctuations around them. An analytical solution of the CME for the self-repressing gene can be obtained when the mRNA variable is considered to be fast and can be eliminated adiabatically (32, 33), but this assumption is unrealistic for the *Hes1* feedback network, where mRNA and protein have similar lifetimes (17). A classical strategy for approximating the CME is the system-size expansion also known as Van Kampen’s Ω -expansion (31). Assuming that the system size is large but not infinite, the solution is expanded in powers of the inverse system size. The deterministic mean-field equations are obtained at lowest order while next-to-leading order corrections determine finite-size fluctuations in the so-called linear noise approximation (LNA). This approach can be used to estimate the amplitude of fluctuations (34) but also to determine their spectrum. In the latter case, the LNA has been useful to characterize the appearance of stochastic oscillations in parameter regions where the mean-field equations predict stable steady behavior (35, 36) or to verify that oscillations predicted by a deterministic modeling persist in presence of fluctuations (37), two problems which has been much studied (38–41). To overcome the fact that this method does not allow one to determine precisely when the steady state loses stability, Scott, Ingalls and Hwa proposed an extension of the LNA which takes into account how fluctuations modify the linearized dynamics around steady state and allows one to study how bifurcation diagrams are modified by noise (42). However, all these methods based on system size expansion assume that fluctuations vanish in the infinite size limit, without affecting the average values. This assumption clearly does not hold when the gene state is a binary variable which fluctuates between two discrete values, regardless of system

size. A different approach must then be taken.

In this paper, we derive a deterministic description of the stochastic dynamics of a basic self-repressing gene circuit, with no cooperativity in the transcriptional regulation and a linear degradation mechanism (Fig. 1A). The gene switches stochastically between the active and inactive state, so that this circuit can be viewed as a random telegraph signal generator, whose output is sent through a low-pass filter before being fed back to itself (Fig. 1B). It is well known that a mean-field model of this system is unconditionally stable (see, e.g., (26)). Our main result is that an ODE model taking fluctuations into account predicts oscillatory behavior in a region of parameter space where we observe relatively regular spiking in protein concentration.

Using a moment closure approximation of the master equation (33, 43, 44), we derive deterministic differential equations which generalize the usual mean-field description while taking into account the binary nature of the gene state variable. These equations describe the combined time evolution of average quantities and of fluctuations around them, and correctly predict the appearance of oscillations, as well as the stationary state value of the network without any assumption on the gene switch time scale nor on the statistical distribution of random variables. We then explain the appearance of stochastic oscillations by a simple resonance effect between the characteristic times scales of the stochastic network and derive an analytical criterion for their appearance. Finally, fitting this criterion with parameter values relevant for the *Hes1* network suggests that the mechanism we describe may be exploited to generate robust oscillations in *Hes1* expression. Our findings highlight the functional role of intrinsic fluctuations arising from the gene state-flip dynamics as an important ingredient for shaping the dynamics of genetic networks.

Results and discussion

Deterministic models taking fluctuations into account

Three stochastic variables characterize the network dynamical state: the gene state g , the mRNA copy number m and the protein copy number p . The time evolution of the probabilities $P_{g,m,p}$ of being in a state with given values of g , m and p is given by the following chemical master equation:

$$\frac{d}{dt}P_{g,m,p} = (-1)^g \left[\frac{k_{on}}{\Omega} (p+1-g) P_{1,m,p+1-g} - k_{off} P_{0,m,p-g} \right] \quad (1a)$$

$$+ \delta_{g,1} \alpha \Omega [P_{g,m-1,p} - P_{g,m,p}] + \beta m [P_{g,m,p-1} - P_{g,m,p}] \quad (1b)$$

$$+ \delta_m [(m+1)P_{g,m+1,p} - mP_{g,m,p}] + \delta_p [(p+1)P_{g,m,p+1} - pP_{g,m,p}] \quad (1c)$$

which can be read from (Fig. 1A) and provides the most general description of the dynamics. The parameters k_{on} and k_{off} characterize the kinetics of protein-DNA binding and unbinding, respectively. The transcription rate and translation rate are α/Ω and β , where Ω represents the cell volume, and δ_m and δ_p are the mRNA and protein degradation rates. The equations are normalized so that in the large volume limit, the average gene activity $\langle g \rangle$ and average concentrations $\langle m \rangle/\Omega$ and $\langle p \rangle/\Omega$ become independent of Ω .

Unfortunately, the master equation has generally no analytical solution. Contrary to the mRNA and protein copy numbers, which become much larger than one in the large volume limit and have then negligible fluctuations when a single molecule is created or destroyed, the gene state is a binary variable and its relative jump size does not decrease. Therefore, the standard approximation method based on the large-volume expansion of the master equation with the van Kampen ansatz fails (31). Alternatively, the chemical master equation can be reformulated as an infinite hierarchy of coupled differential equations whose variables are the joint cumulants of the random variables g , m , and p (31). This strategy leads to deterministic differential equations taking the fluctuations into account and having the mean-field rate equations as a limiting case.

To be specific, let us consider the equations describing the time evolution of the averages of gene activity and mRNA and protein concentrations in the infinite volume limit:

$$\frac{d}{dt}\langle\mathcal{P}\rangle = \beta\langle\mathcal{M}\rangle - \delta_p\langle\mathcal{P}\rangle; \quad (2a)$$

$$\frac{d}{dt}\langle\mathcal{M}\rangle = \alpha\langle g\rangle - \delta_m\langle\mathcal{M}\rangle; \quad (2b)$$

$$\begin{aligned} \frac{d}{dt}\langle g\rangle &= k_{off}[1 - \langle g\rangle] - k_{on}[\langle g\mathcal{P}\rangle], \\ &= k_{off}[1 - \langle g\rangle] - k_{on}[\langle g\rangle\langle\mathcal{P}\rangle + \text{cov}(g, \mathcal{P})], \end{aligned} \quad (2c)$$

where \mathcal{M} (resp., \mathcal{P}) denotes the mRNA (resp., protein) concentration m/Ω (resp. p/Ω), $\langle x\rangle = \sum_{g,m,p} x P_{g,m,p}$ is the average of the stochastic variable x and $\text{cov}(x, y) = \langle xy\rangle - \langle x\rangle\langle y\rangle$ is the covariance of x and y . These equations are derived following the approach described in the Supporting Material. Because of the nonlinear term associated with DNA-protein binding in Eq. (2c), this equation can only be reformulated in terms of the average values $\langle x\rangle$ by introducing the covariance term $\text{cov}(g, P)$. This term does not appear in the usual rate equations describing the kinetics of the self-repressing gene. It describes the feedback from stochastic fluctuations into the dynamics of the average values and plays therefore a key role to model the influence of the gene state-flip dynamics. Eqs. (2) also indicate that the dynamics of mRNA and proteins behaves as a low-pass filter whose input is the mean gene state $\langle g\rangle$ and output is the mean protein concentration $\langle P\rangle$. The cut-off frequency of this low-pass filter depends only on mRNA and protein degradation rates and has a typical value of $\omega_c = \frac{\delta_m\delta_p}{\delta_m + \delta_p}$.

Eqs. (2) are only the first of an infinite hierarchy of equations where time derivatives of the averages are expressed in terms of averages and covariances, the time derivatives of covariances are expressed in terms of covariances and third-order cumulants, and so on (see Supporting Material). In order to truncate this infinite hierarchy to a finite set of equations, a closure approximation must be used. For instance, the usual rate equations are obtained when infinite cell volume and vanishing covariances are assumed (i.e., the $\text{cov}(g, P)$ term in Eqs. (2) is set to 0). The approximation neglects all fluctuations and assumes that all variables have precise values, which conflicts with the binary nature of the gene state. Here, we derive and analyze a higher-order model, named thereafter the Third-Order Truncation (TOT) model, by keeping only three

averages and five covariances as dynamical variables and neglecting all cumulants of order three and greater. This assumes that variables are Gaussian-distributed and that their dynamics can be described by their averages and covariances (45). We also assume infinite cell volume, so that the only remaining fluctuations are those induced by the gene flipping dynamics. In this limit, protein and mRNA copy numbers are also infinite and thus their variation by one unit is negligible, whereas the gene state is a binary variable, whose time evolution is similar to a random telegraph signal.

The TOT model is most conveniently expressed in terms of eight differential equations which specify the time evolution of the averages and covariances of g , p and of a new variable $u = (\beta m + \delta_m p)/(\delta_p + \delta_m)$, after suitable rescaling. More precisely, the equations comprising the TOT model, whose derivation is detailed in the Supporting Material, read

$$\frac{d}{dT}P = \eta(U - P); \quad (3a)$$

$$\frac{d}{dT}U = \Lambda G - P; \quad (3b)$$

$$\frac{d}{dT}G = \rho(1 - G - GP - \Delta_{G,P}); \quad (3c)$$

$$\frac{d}{dT}\Delta_{G,U} = \Lambda G(1 - G) - \Delta_{G,P} - \rho[G\Delta_{P,U} + (P + 1)\Delta_{G,U}]; \quad (3d)$$

$$\frac{d}{dT}\Delta_{G,P} = \eta[\Delta_{G,U} - \Delta_{G,P}] - \rho[G\Delta_{P,P} + (P + 1)\Delta_{G,P}] \quad (3e)$$

$$\frac{d}{dT}\Delta_{U,U} = 2[\Lambda\Delta_{G,U} - \Delta_{P,U}]; \quad (3f)$$

$$\frac{d}{dT}\Delta_{P,P} = 2\eta(\Delta_{P,U} - \Delta_{P,P}); \quad (3g)$$

$$\frac{d}{dT}\Delta_{P,U} = \Lambda\Delta_{G,P} - \Delta_{P,P} + \eta[\Delta_{U,U} - \Delta_{P,U}]. \quad (3h)$$

where P , U , G are the rescaled averages of the random variables p , u and g , and the $\Delta_{X,Y}$ are the corresponding covariances. The three control parameters η , Λ and ρ are defined below.

The dynamics is controlled by three key parameters

The biochemical reaction network of the self-repressing gene (Fig. 1-A) has six independent kinetic parameters. Three parameter combinations represent scales and thus can be taken out of the equations by rescaling time as well as mRNA and protein concentrations. These are : $\frac{k_{off}}{k_{on}}$, which is the protein concentration at which gene is half repressed; $\frac{\delta_p k_{off}}{\beta k_{on}}$ which is the mRNA concentration corresponding to half-repression in steady state; and $\frac{\delta_m + \delta_p}{\delta_m \delta_p}$, which is the response time of the low pass filter. There remain three reduced parameters, denoted below by ρ , Λ , η , which control the dynamics and are discussed below.

The parameter $\rho = k_{off} \frac{(\delta_m + \delta_p)}{\delta_p \delta_m}$ measures the gene unbinding rate relative to the cut-off frequency of the low-pass filter. A low value of ρ indicates that the low-pass filter transmits all the fluctuations of the gene state : the protein concentration time profile displays squared waveforms enslaved to the gene flip.

By contrast, a high value of ρ corresponds to the case where the low-pass filter averages out the gene flip dynamics : protein concentration evolves with small amplitude fluctuations around its mean value.

The second reduced parameter $\Lambda = \frac{\alpha\beta k_{on}}{\delta_m\delta_p k_{off}}$ corresponds to the maximum possible protein concentration relative to the half-repression protein concentration threshold $\frac{k_{off}}{k_{on}}$. Dynamically, Λ characterizes the amplification of the gene telegraph signal sent to the low pass-filter. A low value of Λ ($\Lambda \ll 1$) indicates that the gene remains unbound most of the time; the average period of one gene on/off cycle is essentially the “on” state duration t_{on} . On the contrary, a high value of Λ ($\Lambda \gg 1$) indicates that the gene is repressed most of the time; the period of the gene on/off cycle is essentially the “off” state duration t_{off} , governed by k_{off} . Thus, Λ can also be viewed as characterizing the strength of the feedback from the gene to itself via its protein.

The third parameter $\eta = \frac{(\delta_m + \delta_p)^2}{\delta_p \delta_m}$ characterizes whether the protein and mRNA degradation rates are balanced or not. This indicator reaches a minimum value of 4 for equal degradation rates ($\delta_m = \delta_p$) and goes to infinity as one of the degradation rates becomes negligible compared to the other. It is worth noting that the expressions of all key parameters ρ , Λ , and η are symmetric with respect to exchange of δ_m and δ_p . As a consequence, the dynamical properties are unchanged if the mRNA and protein degradation rates are swapped, a fact which was already noted in (26). To distinguish the two regimes which have identical ρ , Λ and η parameter values but different values of δ_m and δ_p , we will later consider the ratio of protein and mRNA degradation rates $\delta = \delta_p/\delta_m$, with $\eta = (1 + \delta)^2 / \delta$. Obviously, the value of η is unchanged under the transformation $\delta \leftrightarrow 1/\delta$.

The deterministic TOT model reproduces well the time averages of the stochastic dynamics

To assess the influence of stochastic fluctuations of gene state on the dynamics of the self-repressing gene, we first performed stochastic numerical simulations to determine the values of the time averages and covariances of the rescaled random variables G , M , and P (see Methods) as a function of the control parameters. These time averages were then compared to the fixed point values of two truncations of the cumulant equation hierarchy: the rate equation model, defined by Eqs. (2) with the covariance term set to zero, and the TOT model defined by Eqs. (3), where the third-order cumulants have been set to zero. These models are defined by sets of ordinary differential equations, whose fixed points are specified by the values of the variables such that all time derivatives are zero. These fixed points are usually stable and thus reflect the stationary regime, however we shall see later that they may become unstable in some conditions, indicating the appearance of spontaneous oscillations.

Let us first examine how the average gene activity depends on ρ (which characterizes the gene response time scale) and Λ (which characterize feedback strength) when protein and mRNA lifetimes are identical ($\delta = 1$). Gene average activity determined by stochastic simulations is shown in Fig. 2-A. The rate equation model correctly predicts the output of these stochastic simulations only when gene dynamics is fast ($\rho \rightarrow$

∞) or when gene repression is small ($\Lambda \ll 1$) (Fig. 2-B). In contrast to this, the TOT model predicts quantitatively gene average activity in the entire (ρ, Λ) plane (Fig. 2-C), in particular in regions where the rate equation approximation fails.

A more detailed assessment of the TOT model accuracy is provided in Fig. 3, which shows how the time averages and first joint cumulants of G , M , and P evolve with ρ and δ , depending on whether they are computed from stochastic simulations (Fig. 3, left column) or from the fixed point values of the TOT model (Fig. 3, right column). The computations are carried out in the strong feedback (high repression) limit ($\Lambda = 100$). Note that in the rate equation approximation, all averages would be constant and the covariances would vanish. Fig. 3 displays only a subset of components of the TOT model fixed point, from which the other can be obtained with the relations $M^* = P^* = \Lambda G^*$, $\Delta_{MM}^* = \Lambda \Delta_{GM}^*$ and $\Delta_{PM}^* = \Delta_{PP}^*$. An important finding is that ρ is the main parameter controlling the averages, as the curves obtained for various values of δ superimpose remarkably well (Fig. 3-A, left column). This remains approximately true for the covariances and higher-order cumulants, although to a variable extent.

Fig. 3 shows that the fixed point values of the TOT model are in good quantitative agreement with the numerical estimators. Concerning the averages (first order cumulants), the overall shapes of the curves, with a maximum around $\rho = 1$, are very similar and the evolution of this maximum with δ is reproduced (Fig. 3-A). The main discrepancy is that the transition from the fast to the slow gene regime is more abrupt in the TOT model than in stochastic simulations, presumably because higher-order contributions to the averages are neglected. The global evolution of the covariances is also well reproduced, and the values of ρ where Δ_{GP} becomes zero are also well predicted for the different values of δ (Fig. 3-B). Similarly, the variation of Δ_{GM} with δ is captured. (Fig. 3-C). However, the TOT model fixed point values overestimate the covariances Δ_{GM} and Δ_{PP} (Fig. 3-C,D) in the fast gene limit. Still, the asymptotic values of the TOT model steady states (summarized in Table S1 in the Supporting Material) are correctly obtained.

A key assumption of the TOT model is that the third-order joint cumulants $K_{G,M,P}$ and $K_{G,P,P}$ vanish. However, Figs. 3-E,F show that they take rather large values in the stochastic simulations, of the order of Λ , in the slow gene limit. One may thus wonder why the TOT model is so effective in this regime. A careful analysis of the structure of the equations (Eq. S8 in the Supporting Material) solves this paradox. The key point is that in the expressions of the time derivatives of the covariances, the third-order joint cumulant are weighted by ρ so that their dynamical influence vanishes in the slow-gene limit (see Sec. S4 in the Supporting Material). Therefore, the TOT model is a valid approximation for both fast and slow gene dynamics, and provides a reasonable description of the dynamics in the intermediate regime.

Simple dynamical considerations can explain the observed dependency of cumulants on ρ . If $\rho \gg 1$, the gene flip dynamics is averaged by the low pass filter, as previously mentioned, and the stationary regime is correctly predicted by the fixed point values of the rate equations. In this limit, the gene remains bound or unbound for very short amounts of time, during which mRNA and proteins copy numbers can be considered as constant. RNA and protein levels keep a memory of many previous state switching cycles, and reach a

stationary state with a probability distribution which is expected to be Gaussian, as is confirmed by the vanishing of third order cumulants $K_{G,M,P}$ and $K_{G,P,P}$. The coefficient of variation $CV = \frac{\sqrt{\Delta_{PP}^*}}{P^*}$ tends to zero as ρ increased, indicating that fluctuations in protein concentration become negligible compared to the average concentration in the limit of fast gene dynamics ($\rho \rightarrow \infty$). The negative value taken by the covariance Δ_{GP} is consistent with the negative feedback loop structure of the genetic network.

Conversely, if $\rho \ll 1$, the gene reacts infinitely slowly. The dynamics is then driven by the gene jumping between two states according to a Poisson process. During the time where the gene is active (resp. inactive), protein and mRNA levels quickly converge to their maximum value Λ (resp. to zero); at the end of an gene switching state cycle, variables are always in the same state with no memory of previous cycles. This is consistent with the positive value of Δ_{GP} . Protein concentration temporal profiles feature a sequence of squared shape spikes, distributed in time according to a Poisson process, and characterized by a coefficient of variation $CV \approx \sqrt{\Lambda}$ increasing with the overall production rate Λ . Thus, fluctuations are enhanced by a slow gene and a high repression.

Then, a natural question is whether there exists between these two limit cases a dynamical regime which both behaves deterministically, as in the fast-gene limit, and displays strong variations of the protein concentration, as in the slow-gene limit. Such dynamical behavior would feature a sequence of protein concentration spikes, but with a time interval distribution more regular than a Poisson process. This intuition is based on the fact that when the gene flip frequency and the cut-off frequency of the low-pass filter are resonant ($\rho \approx 1$), the random fluctuations of gene flips generated by the Poisson process should be partially buffered by the low-pass filter. This mechanism should prevent spike bunching, generating a more regular dynamical behavior, which would be the stochastic analogue of an oscillatory behavior (that we termed thereafter stochastic oscillations). To assess the veracity of this idea, we developed a criterion to quantify the regularity of stochastic oscillations, described in next section.

Negative feedback induces protein spike antibunching

The regularity of a stochastic oscillatory behavior is often quantified using a temporal autocorrelation function (8, 37, 46). This measure is sensitive to reproducibility both in time and in amplitude. However, temporal regularity is certainly more relevant than amplitude regularity for biological protein signals. The highly nonlinear response of many signaling cascades can protect them against fluctuations in amplitude, for example by saturating output above an input threshold. A standard technique for assessing temporal regularity is to divide the state space into two regions I and II and to study the distribution of the times where the system leaves I to enter II. It is often useful to require a minimal excursion in region II to avoid spurious transitions induced by noise. Here, we detect events where the protein level crosses successively the mean protein level P^* and the $P'^* = P^* + 0.25\sqrt{\Delta_{pp}^*}$ level before falling back below the mean protein level.

Given the list of times where the system transits from low to high protein levels, we compute the

probability of detecting n transitions within a time interval of fixed duration. To be specific, we select a time interval equal to ten times the average time between two events, and characterize the probability distribution of the number of events by the variance to mean ratio, also known as the Fano factor (47). This method is inspired by how the temporal distribution of photons from a light source is generally characterized, with the event of interest being a photon detection. A Fano factor close to unity is obtained when time intervals between events follow a Poisson distribution. A Fano factor greater (less) than unity indicates super-Poissonian (resp., sub-Poissonian) behavior corresponding to a bunching (resp., anti-bunching) of protein spikes. Spike anti-bunching can be viewed as a stochastic counterpart of deterministic oscillations. While using the coefficient of variation of the interspike interval would give similar results, the method described above has the advantage to take into account correlations between the successive transitions.

Figure 3 displays stochastic simulations of the chemical reaction network of Fig. 1 for a slow, an intermediate and a fast gene, as well as the probability distribution of the number n of transitions within a given time window. As expected, protein spikes in the slow gene case (Fig. 3-A) are slaved to the switching process, leading to a Poisson probability distribution for n (Fig. 3-D) and accordingly a unity Fano factor. In the intermediate gene response time case (Fig. 3-B), protein spikes are mostly antibunched (see black circles). The probability distribution of spike number is gaussian-like (Fig. 3-E), the Fano factor being around 0.25. This anti-bunching degrades in the case of a fast gene (Fig. 3-C) with the Fano factor rising to 0.9. Thus, we observe a resonance effect which results from the coincidence of the gene response time to protein variations and the time during which previous gene state history is remembered, which is controlled by the protein and mRNA decay rates.

We studied systematically how the Fano Factor depends on the gene resonance parameter ρ and the relative protein decay rate δ in stochastic simulations (Fig. 5). We found that the regularity of protein spikes is reinforced by (1) similar mRNA and protein decay rates ($\delta \approx 1$), (2) a resonance parameter close to unity ($\rho \approx 1$), and (3) a sufficiently strong feedback ($\Lambda > 1$), as shown in Fig. 5-A,B. Thus, the most regular oscillations are observed when the gene cycling period resonates with the average mRNA/protein lifetime.

The lack of symmetry with respect to the transformation $\delta \leftrightarrow 1/\delta$ for low values of Λ (Fig. 5-B) results from numerical difficulties to reach the infinite cell volume limit for small δ_p ($\delta \ll 1$). As a control, we checked that the Fano Factor is almost independent of the ratio β/δ_p (see Fig. 5-C), which determines the protein to mRNA ratio. This confirms that the reduced parameter Λ is the relevant parameter for describing the overall production rate and thus the amplification factor of the feedback loop.

In the large Λ limit, it is expected that the gene spends most of the time in the “off” state so that the average duration of one “on”/“off” cycle is approximately given by $\tau_{\text{off}} = 1/k_{\text{off}}$ in original time units. To study the interplay between the gene state dynamics and the protein spike dynamics, a useful indicator is $\chi = k_{\text{off}} \langle T_s \rangle$ where T_s is the average time interval between two spikes. In the slow gene limit ($\rho \rightarrow 0$), χ tends to 1, indicating that protein and mRNA are slaved to the gene dynamics in a “fire and degrade”

mode. Conversely, the high value of χ in the fast gene limit indicates that the gene dynamics is too fast to be relevant and justifies an adiabatic elimination of the gene state variable. In the parameter region where spikes are more regular, the intermediate values taken by χ (between 1 and 10) reveals that the gene dynamics and the mRNA/protein dynamics influence each other and generate together the stochastic oscillations observed.

A deterministic model predicts the appearance of stochastic oscillations

If a moment-closure model such as the TOT model (Eqs. (3)) is relevant to the dynamics of the self-repressing gene, it should be able to predict the stochastic oscillations evidenced in the previous section. While such models take fluctuations into account, they are deterministic ODE models, where the natural counterpart of the regular spiking observed in stochastic simulations is the occurrence of self-sustained oscillations. A linear stability analysis of the TOT model should then provide analytical insight into the key parameters controlling the stochastic oscillations.

Because the TOT-model is eight-dimensional, and thus difficult to analyze analytically, we considered a reduced version of it, obtained under the assumption that $\rho \ll \eta, 1$, which corresponds to the slow-gene limit. In this limit, the following subset of equations uncouples from the others, regardless of whether third-order joint cumulants vanish or not (they can be obtained by setting $\rho = 0$ in Eqs. (3)):

$$\frac{d}{dT}P = \eta(U - P); \quad (4a)$$

$$\frac{d}{dT}U = \Lambda G - P; \quad (4b)$$

$$\frac{d}{dT}G = \rho(1 - G - GP - \Delta_{G,P}); \quad (4c)$$

$$\frac{d}{dT}\Delta_{G,U} = \Lambda G(1 - G) - \Delta_{G,P}; \quad (4d)$$

$$\frac{d}{dT}\Delta_{G,P} = \eta[\Delta_{G,U} - \Delta_{G,P}], \quad (4e)$$

Besides the averages, the reduced model (4) incorporates the dynamics of the covariances of the gene state variable with protein and mRNA levels. These are indeed the variables that most directly capture the influence of gene state fluctuations on the dynamics of the self-repressing gene.

Remarkably, a stability analysis of Eqs. (4) reveals that this system exhibits a Hopf bifurcation leading to oscillatory behaviour when the Routh–Hurwitz oscillation criterion

$$\mathcal{H}(\rho, \eta, \Lambda) = \rho^2 \left(\frac{2\Lambda + 1}{\Lambda + 1} \right)^2 + \rho \left[\frac{2\eta\Lambda + \eta - \Lambda^2}{\Lambda + 1} \right] + \eta < 0. \quad (5)$$

is satisfied. Since the mean-field model of the self-repressing gene is unconditionally stable, this shows that fluctuations can play a functional role to promote oscillations. The expression of criterion (5) shows that Λ and η are the key parameters controlling the appearance of oscillations in Eqs. (4) and accordingly of

regular spiking in the stochastic simulations. In particular, it can be seen that the only negative term in (5) is $-\rho\Lambda^2/(\Lambda + 1)$ and thus that a large value of Λ generally favors oscillations. On the other hand a small value of η is required for the criterion (5) to become negative over some range of ρ . More precisely, it is easily shown that the existence of an oscillation region requires that $\Lambda \geq 2\eta + 4\sqrt{\eta}$ (when this inequality is satisfied, the assumption $\Lambda \gg 1$ under which it is derived holds naturally). Whether oscillations actually occur, however, depends on the value of the resonance parameter ρ .

When $\rho \rightarrow 0$ (i.e., the gene cycling period is much longer than average protein/mRNA lifetimes), the criterion is never satisfied because $\mathcal{H} = \eta > 0$, and no oscillations occur. When $\rho \rightarrow \infty$, the dominant term is obviously positive, and no oscillations occur either. For intermediate values of ρ , the quantity \mathcal{H} becomes negative for sufficiently large Λ and for η sufficiently close to its minimum value of 4, as discussed above. Thus, oscillations are favored when feedback is strong and when the mRNA and protein degradation rates are balanced. In the limit of large Λ ($\Lambda \gg \eta$), the criterion (5) simplifies to $\mathcal{H}(\rho, \eta, \Lambda) = 4\rho^2 - \rho\Lambda + \eta < 0$ and oscillations are then found for $\rho \in [\rho_l, \rho_h] = [\eta/\Lambda, \Lambda/8]$, a rather wide interval around $\rho \sim 1$. Note that since $\Lambda \gg \eta$, the lower bound of the oscillation interval is naturally located in the region $\rho \ll 1$ where the reduced model is valid. However, whether oscillations actually occur for larger values of ρ , including the upper bound $\Lambda/8$ is less clear.

Comparing with numerical simulations, we can see in Fig. 5-A,B that the criterion (5) is fairly well satisfied in the region of parameter space where regular stochastic oscillations are observed, especially when the influence of the parameters ρ and δ is considered. On the other hand, while the influence of feedback strength Λ on the appearance of oscillations depending on degradation rate balance is correctly captured, the criterion (5) overestimates the value of Λ where regular oscillations are first observed (Fig. 5-B). The good agreement observed over a wide range of values of ρ is all the more surprising as the reduced model (4) is in principle valid only in the slow gene limit (i.e., for ρ sufficiently small). Indeed, it does not predict correctly the average values when ρ is of order 1 or larger.

To conclude, the reduced model (4) captures well how the mean-field variables and fluctuations interact to generate relatively regular stochastic oscillations, although it does not reproduce satisfactorily the average gene activity over the entire parameter space. This suggests that the joint cumulants involving the gene state are the most dynamically important ones, which is consistent with the fact that the gene state remains a binary variable in all limiting cases and thus is the most stochastic variable.

Oscillations in *Hes1* expression match the criterion for fluctuation-induced oscillations

The main result of this work is that stochastic fluctuations in a self-repressing gene can play a functional role in promoting the appearance of relatively regular oscillations in specific regions of the parameter space. It is then natural to ask whether oscillating self-repressing gene circuits found in biological systems operate in the parameter region we have identified. One such circuit that has been intensively studied is the *Hes1* gene, which is believed to be at the core of the somite clock (17). It is well known that a crucial ingredient

of oscillations in *Hes1* expression is the presence of a time delay, associated to transcription, translation or transport. This time delay is often modeled as an explicit time delay (23–25, 40), however it can also result from a slow reactional step (21, 22, 26).

In our system, the time delay is due to the finite gene response time related to the binding/unbinding dynamics. This finite gene response time can also be viewed as taking into account phenomenologically other sources of delay, if they arise from reactional steps and thus are exponentially distributed. More precisely, the gene can persist in the “off” state for some time after protein level goes down because of the characteristic time $\tau_g = k_{off}^{-1}$ (in original time units) needed to switch from the “off” to the “on” state. Therefore, this characteristic time can be viewed as the delay inducing oscillations, and large-scale variations of protein concentration will typically appear when it is not too small compared to protein half-life. We found that these variations are more regular when these two time scales are equal. Of course, the oscillations in our model remain less regular than those observed in *Hes1* because, (1) the delay is exponentially distributed rather than constant and (2) there is no cooperativity. Yet, the models are sufficiently similar that if there is a parameter region where fluctuations promote oscillations in our stochastic self-repressing gene model, this should remain true for the *Hes1* circuit since oscillations would then be more robust to random variations of the delay. Such random variations could be due for instance to the presence of reactional steps. We should then expect this specific parameter region to be selected by evolution.

A first interesting observation is that in the *Hes1* oscillator, the protein and mRNA half-lives are approximately equal, with reported values of 22 and 24 minutes, respectively (17). This is fully consistent with both our observation that regular oscillations occur preferably for $\delta = 1$ (Fig. 5) and the fact that the oscillation criterion (5) for the 5-variable reduced model (4) indicates that η should be as close as possible to its minimum, which corresponds to balanced half-lives. Note that this contrasts markedly with what is known for the mean-field model, where making degradation rates unbalanced while keeping their sum constant favors oscillations (26).

A crucial parameter for the regularity of the stochastic oscillations is the resonance parameter ρ , which depends on the time delay and on the mRNA and protein half-lives. However, the time delay in the *Hes1* circuit is not known experimentally. In theoretical investigations (see, e.g., (40, 48)), it is generally assumed that the time delay ranges from 10 to 40 minutes. We assume here a value of 30 minutes, which is consistent with the fact that for large half-lives, the oscillation period of 120 minutes is approximately equal to four times the delay according to Lewis (23). With the known values for the mRNA and protein half-lives (which translate to $\delta_p \sim \delta_m \sim 0.3$), this yields $\rho \sim 2$. Together with $\delta = 1$, this value corresponds precisely to the region of regular oscillations in Fig. 5A. Furthermore, note that Fig. 5D indicates that for $\rho = 2$, the ratio of the oscillation period to the delay $1/k_{off}$ is indeed close to 4.

Finally, other theoretical investigations (see, e.g., (40, 48)) assume that $\Lambda \gg 1$. This in fact a natural condition, which simply requires that the maximum protein level reached when the gene is fully active must be much larger than the half-repression threshold. This ensures that the protein level can go below and

above this threshold in the course of oscillations, and that the gene is strongly repressed when protein level is high.

Taken together, these facts strongly suggest that the *Hes1* mRNA and protein half-lives have been tuned to be both close to the time delay in order to make oscillations in *Hes1* expression robust against stochastic fluctuations in delay.

Conclusion

In this paper, we have studied the stochastic dynamics of a simple self-repressing gene model, in which the gene switches randomly between the active and inactive state with a characteristic time which can be arbitrarily small or large compared to mRNA and protein lifetimes. The regularity of the protein spikes generated by the dynamics was characterized using a Fano-like indicator. This allowed us to evidence a dynamical resonance phenomenon, namely that a more regular time evolution of protein concentration is observed for certain values of the protein to mRNA degradation rate ratio and of the gene response time. It should be stressed that there is neither cooperativity nor nonlinear degradation in our model, so that the regularity of the oscillations displayed in Fig. 4B could easily be improved by using these two ingredients, as is done in most theoretical investigations, or by considering a fixed time delay in addition to the exponentially-distributed gene response time.

To understand the resonance phenomenon, we developed a deterministic ODE model using a moment-closure approximation of the master equation. This model describes the combined time evolution of the averages and covariances of protein, mRNA and gene activity. Thus, it allows us to describe how nonlinearity injects fluctuations into the average dynamics, which can be substantially modified. The steady state of this model predicts well how averages and covariances vary with the gene response time and the ratio of mRNA and protein degradation rates. In particular, it reproduces the fact that the average gene activity is significantly reduced in the slow gene limit. In this limit, a 5-dimensional model can be obtained, which incorporates the three averages and the two covariances of the gene state with the protein and mRNA concentrations. This model displays a Hopf bifurcation which is not present in the mean-field model. Remarkably, the parameter region where the reduced model oscillates matches the region where the protein spikes are more regularly spaced, even though the model predicts correct steady-state values only in the slow gene limit. Therefore, deriving deterministic equations through a moment-closure approximation of the master equation appears to be an effective approach to describe the bifurcation diagram of stochastic dynamical systems, which is generally a difficult problem (see, e.g., (49, 50)). This approach is all the more interesting as computer software is available to derive the hierarchy of equations for the cumulants of increasing order (43, 51). The approach describe here is well fitted to problems where one variable remains microscopic, such as gene state, and where fluctuations dramatically affect the average values. It thus brings a distinctive advantage compared to other methods based on the linear noise approximation (42).

To check whether the resonance effect discussed here is relevant in real genetic oscillators, we examined the timescales reported for the *Hes1* self-repressing gene (17, 23, 24). In this circuit, the mRNA and protein lifetimes are approximately equal to the time delay. We found that this situation is characterized by the reduced parameters $\rho = 2$, $\delta = 1$, which correspond precisely to the center of the parameter region where regular protein spiking is observed. This strongly suggests that the phenomenon of stochastic resonance we have unveiled plays an important role for generating robust genetic oscillations, independently of other oscillation-enhancing effects such as cooperativity in the transcriptional regulation (52) or nonlinear degradation (26, 29), which can be simultaneously harnessed. A possibly related observation by Murugan and Kreiman is that protein response times fluctuate less when mRNA and protein lifetimes are closer (53). More generally, we believe that our findings provide a remarkable example of how stochastic fluctuations, which are unavoidable in genetic networks, may play a functional role to shape their dynamics (7).

Methods

To assess the validity of the various truncation schemes, we performed numerical stochastic simulations of the chemical network (Fig. 1-A) for various values of ρ , Λ , and δ . To enforce a one-to-one relationship between the original parameter space $\{k_{on}, k_{off}, \beta, \alpha, \delta_m, \delta_p\}$ and the reduced parameter space $\{\rho, \Lambda, \eta\}$, three constraints are required. So we fixed (1) the ratio $\beta/\delta_p = 10$ to enforce a protein concentration 10 times bigger than mRNA concentration, which is a realistic assumption for a biological network, (2) the repression threshold of the gene $\Omega k_{off}/k_{on} = 100$ to be consistent with the assumption of infinite cell volume while keeping computational time within reasonable limits, (3) $\delta_m = 1$ to set the time scale to the mRNA half-life. Since stochastic simulations deal with copy numbers instead of concentration, the cell volume has no influence and we fixed $\Omega = 1$. The validity of the truncation schemes investigated can then be assessed by comparing the values of the averages in the stochastic simulation with the fixed point values of the ODE models obtained by truncating the cumulant expansion.

The stochastic simulations were performed using an implementation of the next reaction method (Gibson-Bruck algorithm (54)). The time interval used for the numerical estimation of joint cumulants was chosen to ensure a relative error of the estimator of the mean of the gene state smaller than 10^{-4} by monitoring the convergence of the estimator and its fluctuations. To compute an numerical estimation of the Fano factor, we recorded 4000 interspike intervals after a transient whose duration was chosen by the monitoring the convergence of the estimator for the average.

Acknowledgments

This work has been supported by Ministry of Higher Education and Research, Nord-Pas de Calais Regional Council and FEDER through the Contrat de Projets État-Région (CPER) 2007–2013, as well as by LABEX

CEMPI (ANR-11-LABX-0007). The authors thank Benjamin Pfeuty for careful reading of the manuscript.

References

- [1] Hartwell, L., J. Hopfield, S. Leibler, and A. Murray, 1999. From molecular to modular cell biology. *Nature* 402:C47–C52.
- [2] Golding, I., J. Paulsson, S. M. Zawilski, and E. C. Cox, 2005. Real-time kinetics of Gene activity in Individual bacteria. *Cell* 113:1025–1036.
- [3] Darzacq, X., Y. Shav-Tal, V. de Turriz, Y. Brody, S. M. Shenoy, R. D. Phair, and R. H. Singer, 2007. In vivo dynamics of RNA polymerase II transcription. *Nat. Struct. Mol. Biol.* 14:796–806.
- [4] Chubb, J. R., T. Trcek, S. M. Shenoy, and R. H. Singer, 2006. Transcriptional Pulsing of a Developmental Gene. *Curr. Biol.* 16:1018–1025.
- [5] Suter, D. M., N. Molina, D. Gatfield, K. Schneider, U. Schibler, and F. Naef, 2011. Mammalian Genes Are Transcribed with Widely Different Bursting Kinetics. *Science* 332:472–474. <http://www.sciencemag.org/content/332/6028/472.abstract>.
- [6] Harper, C. V., B. Finkenstdt, D. J. Woodcock, S. Friedrichsen, S. Semprini, L. Ashall, D. G. Spiller, J. J. Mullins, D. A. Rand, J. R. E. Davis, and M. R. H. White, 2011. Dynamic Analysis of Stochastic Transcription Cycles. *PLoS Biol* 9:e1000607. <http://dx.doi.org/10.1371/journal.pbio.1000607>.
- [7] Eldar, A., and M. Elowitz, 2010. Functional roles for noise in genetic circuits. *Nature* 467:167–273.
- [8] Simpson, M. L., C. D. Cox, and G. S. Sayler, 2003. Frequency domain analysis of noise in autoregulated gene circuits. *Proceedings of the National Academy of Sciences* 100:4551–4556. <http://www.pnas.org/content/100/8/4551.abstract>.
- [9] Warren, P. B., S. Tanase-Nicola, and P. R. ten Wolde, 2006. Exact results for noise power spectra in linear biochemical reaction networks. *The Journal of Chemical Physics* 125:144904. <http://link.aip.org/link/?JCP/125/144904/1>.
- [10] Lestas, I., J. Paulsson, N. Ross, and G. Vinnicombe, 2008. Noise in gene regulatory networks. *Automatic Control, IEEE Transactions on* 53:189–200.
- [11] Aquino, T., E. Abranches, and A. Nunes, 2012. Stochastic single-gene autoregulation. *Phys. Rev. E* 85:061913. <http://link.aps.org/doi/10.1103/PhysRevE.85.061913>.
- [12] Stricker, J., S. Cookson, M. R. Bennett, W. H. Mather, L. S. Tsimring, and J. Hasty, 2008. A fast, robust and tunable synthetic gene oscillator. *Nature* 456:516–520.
- [13] Hermsen, R., B. Ursem, and P. R. ten Wolde, 2010. Combinatorial Gene Regulation Using Autoregulation. *PLoS Comput Biol* 6:e1000813. <http://dx.doi.org/10.1371/journal.pcbi.1000813>.

- [14] Salgado, H., A. Santos-Zavaleta, S. Gama-Castro, D. Milln-Zrate, E. Daz-Peredo, F. Snchez-Solano, E. Prez-Rueda, C. Bonavides-Martnez, and J. Collado-Vides, 2001. RegulonDB (version 3.2): transcriptional regulation and operon organization in *Escherichia coli* K-12. *Nucleic Acids Research* 29:72–74. <http://nar.oxfordjournals.org/content/29/1/72.abstract>.
- [15] Keseler, I. M., J. Collado-Vides, S. Gama-Castro, J. Ingraham, S. Paley, I. T. Paulsen, M. Peralta-Gil, and P. D. Karp, 2005. EcoCyc: a comprehensive database resource for *Escherichia coli*. *Nucleic Acids Research* 33:D334–D337. http://nar.oxfordjournals.org/content/33/suppl_1/D334.abstract.
- [16] Novak, B., and J. J. Tyson, 2008. Design principles of biochemical oscillators. *Nat. Rev. Mol. Cell Biol.* 9:981–991.
- [17] Hirata, H., S. Yoshiura, T. Ohtsuka, Y. Bessho, T. Harada, K. Yoshikawa, and R. Kageyama, 2002. Oscillatory expression of the bHLH factor Hes1 regulated by a negative feedback loop. *Science* 298:840–843.
- [18] Goodwin, B. C., 1965. Oscillatory behavior of enzymatic control processes. *Adv. Enzyme Regul.* 3:425–439.
- [19] Griffith, J. S., 1968. Mathematics of cellular control processes I. Negative feedback to one gene. *J. Theor. Biol.* 20:202–208.
- [20] Bliss, R. D., P. R. Painter, and A. G. Marr, 1982. Role of feedback inhibition in stabilizing the classical operon. *J. Theor. Biol.* 97:177–193.
- [21] Goldbeter, A., 1995. A model for circadian oscillations in the *Drosophila* period protein (PER). *Proc. R. Soc. Lond. B* 261:319–324.
- [22] Leloup, J.-C., D. Gonze, and A. Goldbeter, 1999. Limit cycle models for circadian rhythms based on transcriptional regulation in *Drosophila* and *Neurospora*. *J. Biol. Rhythms* 14:433–448.
- [23] Lewis, J., 2003. Autoinhibition with transcriptional delay: a simple mechanism for the zebrafish somitogenesis oscillator. *Curr. Biol.* 13:1398–1408.
- [24] Monk, N. A. M., 2003. Oscillatory expression of Hes1, p53 and NK- κ B driven by transcriptional time delays. *Curr. Biol.* 13:1409–1413.
- [25] Jensen, M. H., K. Sneppen, and G. Tiana, 2003. Sustained oscillations and time delays in gene expression of protein Hes1. *FEBS Lett.* 541:176–177.
- [26] Morant, P.-E., Q. Thommen, F. Lemaire, C. Vandermoëre, B. Parent, and M. Lefranc, 2009. Oscillations in the Expression of a Self-Repressed Gene Induced by a Slow Transcriptional Dynamics. *Phys. Rev. Lett.* 102:068104. <http://link.aps.org/doi/10.1103/PhysRevLett.102.068104>.

- [27] Tiana, G., S. Krishna, S. Pigolotti, M. H. Jensen, and K. Sneppen, 2007. Oscillations and temporal signalling in cells. *Phys. Biol.* 4:R1–R17.
- [28] Mengel, B., A. Hunziker, L. Pedersen, A. Trusina, M. H. Jensen, and S. Krishna, 2010. Modelling oscillatory control in NF-kB, p53, and Wnt signaling. *Current Opinion in Genetics and Development* 20:656–664.
- [29] Tyson, J. J., C. I. Hong, C. D. Thron, and B. Novak, 1999. A simple model of circadian rhythms based on dimerization and proteolysis of PER and TIM. *Biophys. J.* 77:2411–2417.
- [30] François, P., and V. Hakim, 2005. Core genetic module: the mixed feedback loop. *Phys. Rev. E* 72:031908.
- [31] van Kampen, N. G., 2007. Stochastic processes in physics and chemistry. Elsevier.
- [32] Hornos, J. E. M., D. Schultz, G. C. P. Innocentini, J. Wang, A. M. Walczak, J. N. Onuchic, and P. G. Wolynes, 2005. Self-regulating gene: An exact solution. *Phys. Rev. E* 72:051907.
- [33] Grima, R., D. Schmidt, and T. Newman, 2012. Steady-state fluctuations of a genetic feedback loop: An exact solution. *J. Chem. Phys.* 137:035104.
- [34] Elf, J., and M. Ehrenberg, 2003. Fast evaluation of fluctuations in biochemical networks with the linear noise approximation. *Genome Res.* 13:2475–2484.
- [35] McKane, A. J., and T. J. Newman, 2005. Predator-prey cycles from resonant amplification of demographic stochasticity. *Phys. Rev. Lett.* 94:218102.
- [36] McKane, A. J., J. D. Nagy, T. J. Newman, and M. O. Stefanini, 2007. Amplified biochemical oscillations in cellular systems. *J. Stat. Phys.* 128:165–191.
- [37] Galla, T., 2009. Intrinsic fluctuations in stochastic delay systems: Theoretical description and application to a simple model of gene regulation. *Phys. Rev. E* 80:021909.
- [38] Loinger, A., and O. Biham, 2007. Stochastic simulations of the repressilator circuit. *Phys. Rev. E* 76:051917.
- [39] Blossey, R., L. Cardelli, and A. Phillips, 2008. Compositionality, stochasticity, and cooperativity in dynamic models of gene regulation. *HFSP Journal* 2:17–28.
- [40] Barrio, M., K. Burrage, A. Leier, and T. Tian, 2006. Oscillatory regulation of *hes1*: Discrete stochastic delay modelling and simulation. *PLoS Comput. Biol.* 2:1017–1030.
- [41] Lepzelter, D., H. Feng, and J. Wang, 2010. Oscillation, cooperativity, and intermediates in the self-repressing gene. *Chem. Phys. Lett.* 490:216.

- [42] Scott, M., T. Hwa, and B. Ingalls, 2007. Deterministic characterization of stochastic genetic circuits. *Proc. Nat. Acad. Sci. USA* 104:7402–7407.
- [43] Gillespie, C. S., 2009. Moment-closure approximations for mass action models. *IET Syst. Biol.* 3:52–58.
- [44] Lee, C. H., K.-H. Kim, and P. Kim, 2009. A moment closure method for stochastic reaction networks. *J. Chem. Phys.* 130:134107. <http://link.aip.org/link/?JCP/130/134107/1>.
- [45] Lafuerza, L. F., and R. Toral, 2010. On the Gaussian approximation for Master Equations. *J. Stat. Phys.* 140:917–933.
- [46] Coulon, A., O. Gandrillon, and G. Beslon, 2010. On the spontaneous stochastic dynamics of a single gene: complexity of the molecular interplay at the promoter. *BMC systems biology* 4:2.
- [47] Fano, U., 1947. Ionization yield of radiation .2. The fluctuations of the number of ions. *Phys. Rev.* 72:26–29.
- [48] Bernard, S., B. Cajavec, L. Pujol-Menjouet, M. Mackey, and H. Herzel, 2006. Modelling transcriptional feedback loops: the role of Gro/TLE1 in Hes1 oscillations. *Phil. Trans. R. Soc. A* 364:1155–1170.
- [49] Bratsun, D., D. Volfson, L. S. Tsimring, and J. Hasty, 2005. Delay-induced stochastic oscillations in gene regulation. *Proc. Nat. Acad. Sci. USA* 102:14593–14598. <http://www.pnas.org/content/102/41/14593.abstract>.
- [50] Song, C., H. Phenix, V. Abedi, M. Scott, B. P. Ingalls, M. Krn, and T. J. Perkins, 2010. Estimating the Stochastic Bifurcation Structure of Cellular Networks. *PLoS Comput. Biol.* 6:e1000699. <http://dx.doi.org/10.1371/journal.pcbi.1000699>.
- [51] Vidal, S., M. Petitot, F. Boulier, F. Lemaire, and C. Kuttler, 2012. Models of Stochastic Gene Expression and Weyl Algebra. In K. Horimoto, M. Nakatsui, and N. Popov, editors, Algebraic and Numeric Biology, Springer Berlin Heidelberg, volume 6479 of *Lecture Notes in Computer Science*, 76–97. http://dx.doi.org/10.1007/978-3-642-28067-2_5.
- [52] Purcell, O., N. J. Savery, C. S. Grierson, and M. di Bernardo, 2010. A comparative analysis of synthetic genetic oscillators. *J. R. Soc. Interface* 7:1503–1524. <http://rsif.royalsocietypublishing.org/content/7/52/1503.abstract>.
- [53] Murugan, R., and G. Kreiman, 2011. On the Minimization of Fluctuations in the Response Times of Autoregulatory Gene Networks. *Biophys. J.* 101:1297–1306.
- [54] Gibson, M. A., and J. Bruck, 2000. Efficient Exact Stochastic Simulation of Chemical Systems with Many Species and Many Channels. *J. Phys. Chem. A* 104:1876–1889.

Figure Legends

Figure 1.

Schematic view of the self-repressing gene network. (A) Biochemical reactions composing the network. P , M , G , and $G : P$ denote protein, mRNA, free gene and bound gene chemical species, respectively. The kinetic constants of the reactions are indicated, with Ω denoting cell volume. In the limit where Ω is large, the mRNA and protein copy numbers become macroscopic variables, with decreasing fluctuations, while the gene state remains microscopic and displays full-scale variations. (B) Block diagram representation of the network, consisting of a random telegraph signal generator representing the gene state-flip dynamics, and of a low-pass filter of cut-off frequency ω_c representing proteins and mRNA dynamics. The telegraph signal regulates its frequency and duty cycle through feedback from the low pass filter.

Figure 2.

Average gene activities as a function of the Λ and ρ parameter (A) Numerical estimation of $\langle g \rangle$ using stochastic simulations with parameter values $k_{off}/k_{on} = 100$, $\delta = 1$, $\beta/\delta_p = 10$. (B) Average gene activity predicted by rate equation (C) Fixed point value of gene activity in model (3).

Figure 3.

Comparison of statistical quantities such as averages, covariants and higher-order cumulants obtained from stochastic simulations (left column) and from the TOT model (right column) as functions of parameter ρ , for various values of δ . (A) Average G ; (B), (C) and (D) covariances Δ_{GP} , Δ_{GM} and Δ_{PP} ; (E), and (F) third-order joint cumulants K_{GMP} and K_{GPP} . Curves for different values of δ are color-coded according to legend box. The value of $\Lambda = 100$ used in the simulations corresponds to strong feedback (strong gene repression). Stochastic simulations are performed while constraining $k_{off}/k_{on} = 100$ and $\beta/\delta_p = 10$ (see text for details). In each panel, thick lines (resp., thin) lines indicate positive (resp., negative) values.

Figure 4.

Protein spike antibunching. (A,B,C). Time evolution of protein copy number for $\Lambda = 100$, $\delta = 1$ and $\rho = 10^{-3}$, 1 , 10^3 , respectively. Dashed lines indicate mean protein level and mean protein level plus standard deviation. Black lines correspond to the high trigger level and spiking events are indicated by black circles. (D, E, F) Probabilities of observing n spikes during a time window of 10 averaged transition $\rho = 10^{-3}$, 1 , 10^3 , respectively.

Figure 5.

Regularity of stochastic oscillations In (A), (B), and (C), the value of the Fano factor F , which quantifies spiking regularity, is shown as a function of two parameters using a gray-scale color code with level lines displayed in red. The white lines in (A) and (B) enclose the region where the reduced model (4), discussed in Sec. , predicts oscillations. The regularity of stochastic oscillations is favored by balanced protein and mRNA degradation rates (corresponding to $\delta \simeq 1$) as well as (A) a resonance parameter ρ close to 1, (B) a high value of the overall production rate Λ . (C) The ratio β/δ controlling the relative mRNA to protein concentration has no effect on spike regularity. (D) The oscillation period (or protein average interspike time interval) is controlled by the resonance parameter ρ . The variation of χ , the average number of “on”/“off” cycles in an interspike interval, is displayed using a gray color code as a function of the lifetime ratio δ and of the resonance parameter ρ . Level lines are displayed in red (color online). Stochastic simulations of the biochemical network have been carried out with $k_{off}/k_{on} = 100$; $\beta = 10\delta$ (A, B, and D); $\rho = 1$ (B and C); $\Lambda = 100$ (A, B, and C).

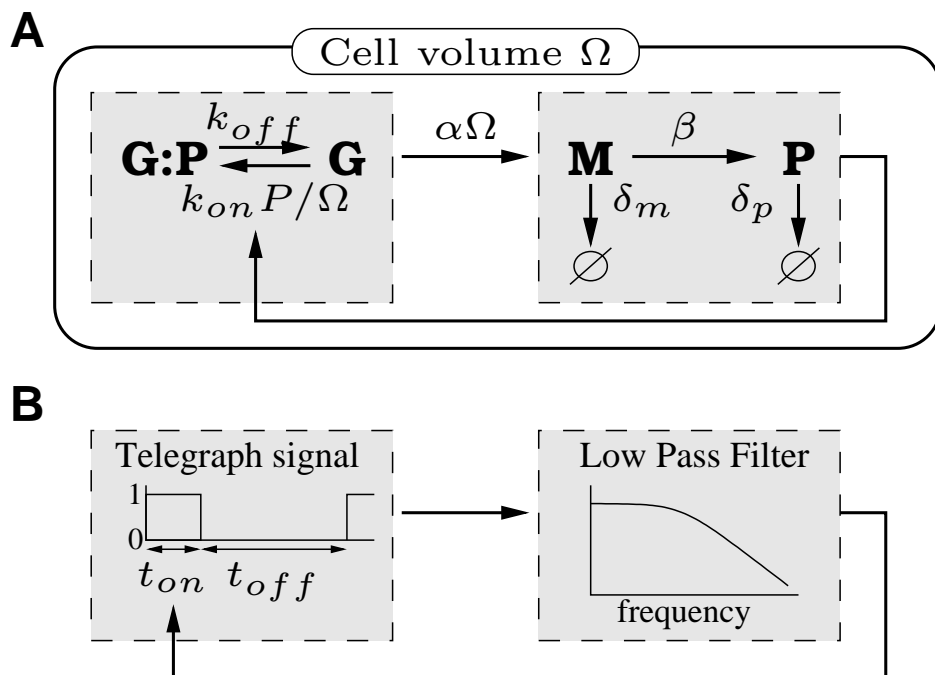


Figure 1:

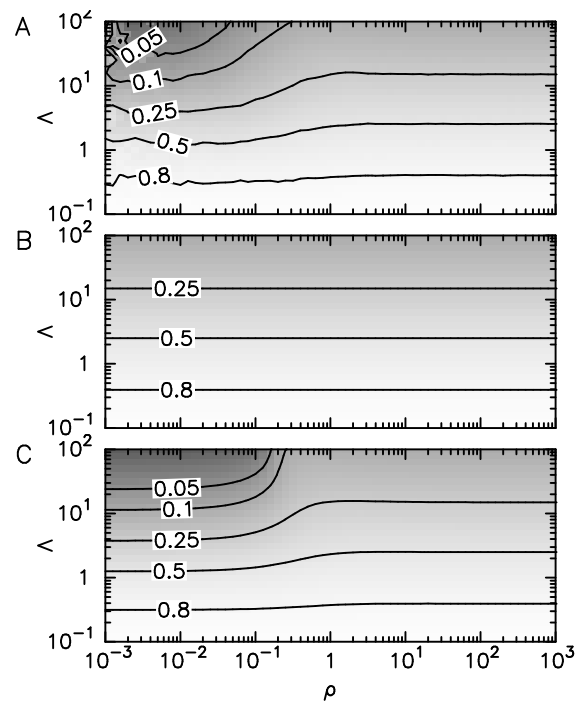


Figure 2:

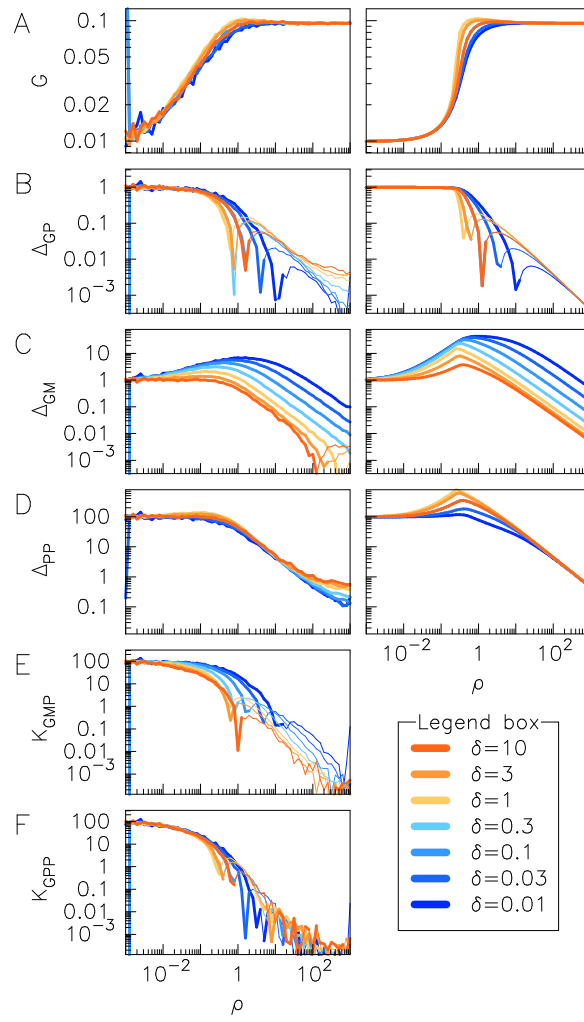


Figure 3:

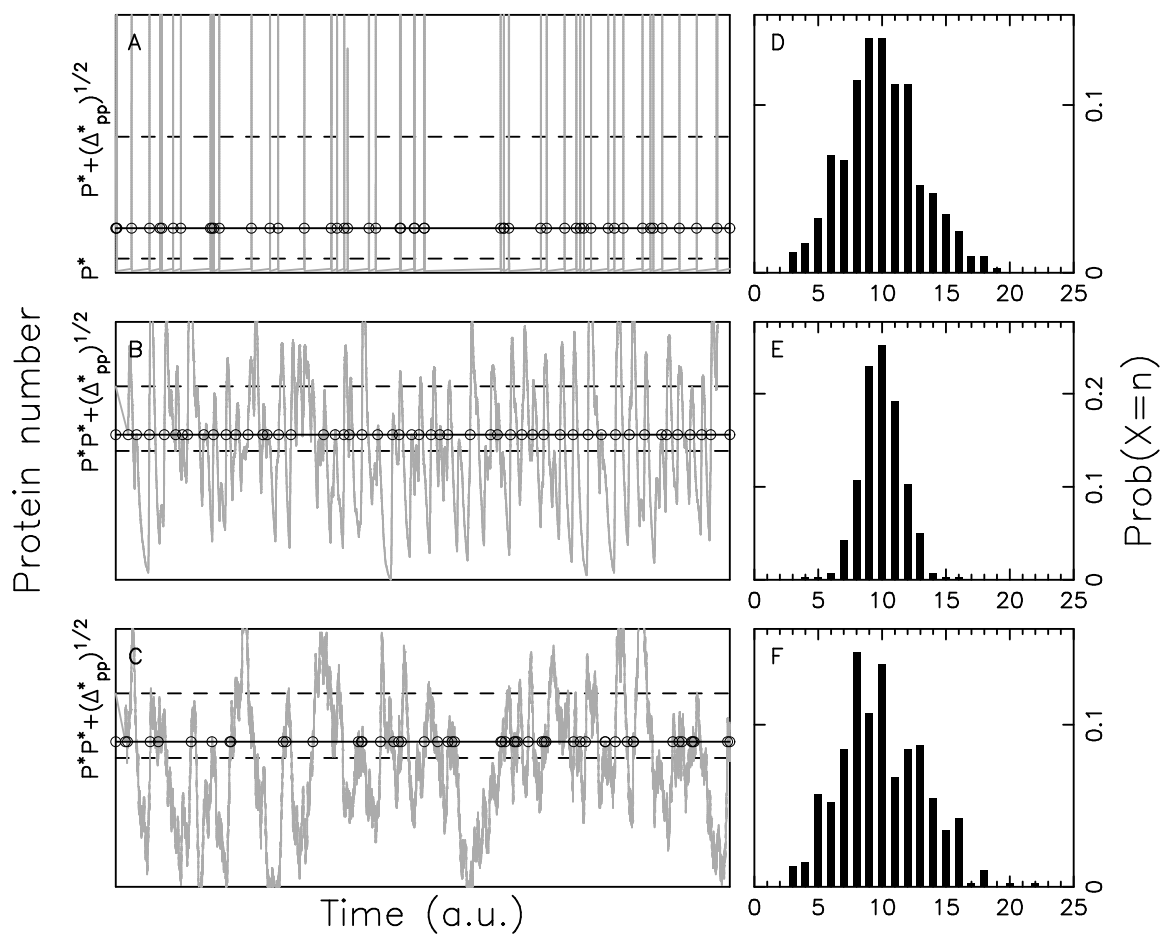


Figure 4:

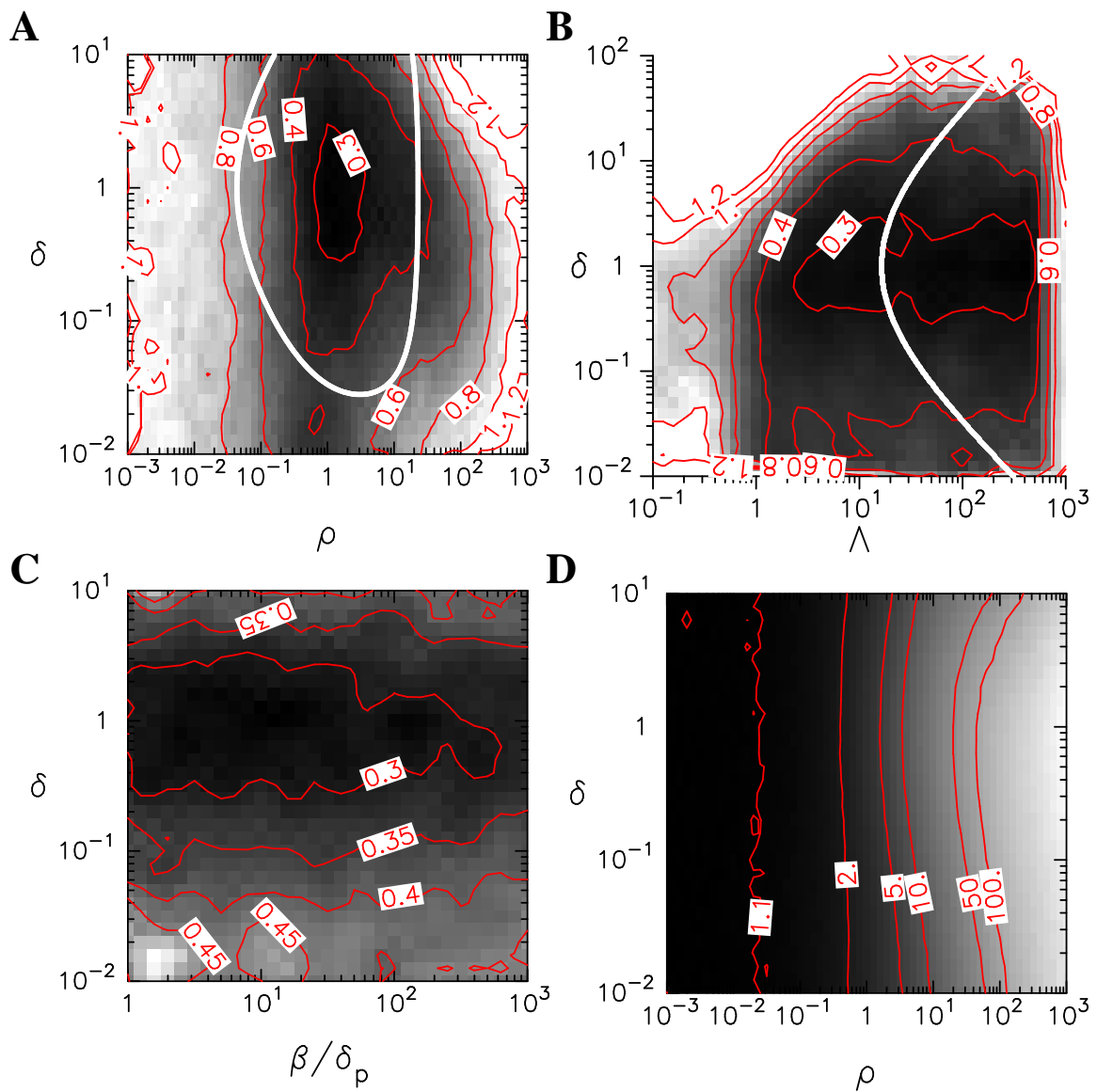


Figure 5: